

**Bioinspired multi-responsive soft actuators controlled by
laser tailored graphene structures**

Journal:	<i>Journal of Materials Chemistry B</i>
Manuscript ID	TB-COM-05-2018-001285.R1
Article Type:	Communication
Date Submitted by the Author:	30-Jul-2018
Complete List of Authors:	Deng, Heng; University of Missouri, Mechanical & Aerospace Engineering Zhang, Cheng; University of Missouri, Mechanical & Aerospace Engineering Su, Jheng-Wun; University of Missouri Columbia, Mechanical & Aerospace Engineering Xie, Yunchao; University of Missouri, Mechanical & Aerospace Engineering Zhang, Chi; University of Missouri, Mechanical & Aerospace Engineering Lin, Jian; University of Missouri-Columbia, Mechanical & Aerospace Engineering

Bioinspired multi-responsive soft actuators controlled by laser tailored graphene structures

Heng Deng, Cheng Zhang, Jheng-Wun Su, Yunchao Xie, Chi Zhang, and Jian Lin*

Department of Mechanical & Aerospace Engineering, University of Missouri-Columbia, Columbia, Missouri 65211, USA.

E-mail: LinJian@missouri.edu

Abstract

By exploiting the aligned cellulose fibrils as geometrically constraining structures, plants can achieve complex programmable shape change upon environment stimuli. Inspired by this natural prototype, a series of manmade materials with aligned structures have been developed and employed in self-morphing materials. However, in these cases, the constraining materials are fabricated and aligned in separate processes. While in the botanic systems, a more efficient way is adopted, in which the aligned microstructures are simultaneously synthesized and aligned in one bottom-up process. Herein, we report a bioinspired bottom-up approach to fabricate laser induced graphene (LIG) structures which resemble the aligned microstructures of the cellulose fibrils in the plants. Such LIG structures serve as geometrically constraining materials to precisely control the shape changing behaviors of soft actuators made from polymer and LIG layers. Meanwhile, LIG structures also serve as functional materials to absorb photo and electrical energy to stimulate motions of the soft actuators. Taking advantages of the geometrically constraining effect from the aligned LIG structures, a series of programmable actuations stimulated by electricity, light, organic vapor, and moisture were demonstrated. Furthermore, the soft actuators also act as soft grippers and walking robots upon different stimuli, indicating their potential applications in soft robotics, electronics, microelectromechanical systems, and others.

Manipulation of structure-property relationship is always the center of study in materials science. Plants are the great masters in such manipulation. They can generate diverse responsive mechanical motions by organizing their internal microstructures. For example, the plants synthesize and align stiff fibrils (cellulose fibrils) within the extracellular matrices of seed dispersal units.¹⁻³ The cellulose fibrils, serving as aligned and constraining structures, restrict the microscopic expansion or shrinkage of the surrounding matrix in the alignment direction of these stiff fibrils while in the transversal direction the shape change is relatively easier due to less structural constraining. Thus, the anisotropic expansion or shrinkage is manifested as macroscopic deformation such as bending and twisting to show functions such as dispersing their seeds.⁴ Inspired by this prototype in nature, enthusiasm of fabricating self-morphing materials to resemble the above biological structures has continued to grow in recent decades.

In an attempt to mimic these natural systems, it is critical to fabricate and align the constraining structures. Until now, manmade materials such as Al_2O_3 platelets,⁴ iron oxide nanoparticle,⁵ liquid crystal,⁶ cellulose fibers,⁷ carbon nanotube,⁸ glass fiber⁹ and latex microspheres¹⁰ have served as the stiff and constraining elements in the matrix of soft materials. By alignment techniques such as magnetic alignment,⁵ photo alignment,⁶ 3D printing,⁷ mechanical spinning alignment,⁸ manual alignment⁹, alternating current (AC) electric alignment¹⁰ these stiff elements are readily aligned to long-range order structures, which can constrain the expansion or shrinkage of the surrounding soft matrix in the alignment direction for programming their macroscopic shape transformations. Despite their ability of generating programmable movement, existing methods of forming the constraining

alignment structures fundamentally differ from the processes employed by the plants in the following distinct ways. In the most cases of synthetic systems, the aligned and constraining elements are processed in separate processes. They are firstly synthesized by methods such as wet chemistry or chemical vapor deposition (CVD),^{5, 6, 11} and then patterned and aligned through the aforementioned alignment techniques. But the plants adopt a more efficient way to generate the alignment of the constraining elements. In the plants, the constraining elements (*e.g.* cellulose fibrils) were directly synthesized from raw materials (*e.g.* uridine diphosphate glucose (UDPG)) and then simultaneously aligned in the same step (Fig. 1a).^{12, 13} If this bioinspired bottom-up approach was adopted in the synthetic systems, the fabrication process would be greatly simplified.

Recently, the direct laser writing (DLW) method has emerged as a novel technique for fabricating micro- and nano- structures with low cost, high efficiency, and flexible designability. Compared to conventional fabrication methods, the DLW can simultaneously synthesize and pattern a series of functional materials such porous graphene,¹⁴ carbon fiber,¹⁵ FeNi alloy,¹⁶ nanodiamond,¹⁷ and MoS₂,¹⁸ directly from their corresponding precursors. Moreover, orientation of these laser induced materials can be delicately tailored by adjusting the direction of laser scanning pathways.¹⁹ In this case, DLW can fabricate aligned microstructures by consuming the starting materials in the same step (Fig. 1b), which resembles the botanic process of directly transforming UDPG into the aligned cellulose fibers. However, to the best of our knowledge, such a laser induction process for fabricating self-morphing materials has yet been demonstrated.

To conceptually verify this idea, we adopted the DLW technique for fabricating aligned

porous graphene as a stiff constraining element for multi-responsive soft actuators with programmable shape transformation. The aligned laser induced graphene (LIG) patterns were fabricated by a one-step DLW, and then sandwiched by active polymers (e.g. poly(vinylidene fluoride) (PVDF)) and passive polymers (e.g. polyimide (PI)) to form PVDF/LIG/PI (PLP) actuators. In this sandwich structure, the PVDF serves as an active layer due to its large coefficient of thermal expansion and strong swelling ability toward organic solvents,^{20, 21} while the PI tape functions as a passive layer because of its low thermal or solvent-induced expansion. The aligned LIG in here possess two functions: (1) serving as a geometrically constraining element to restrain the expansion of the PVDF films in the alignment direction, which resembles the function of the cellulose fibrils in the plants; (2) converting light and electricity to thermal energy for stimulating expansion of the PVDF, endowing the resulting self-morphing materials with capability of remote electric and photonic control. As a result, electrothermal and photothermal actuations were realized in this LIG based soft actuator. In addition, PVDF has high swelling to solvents, the fabricated actuators are responsive to chemical stimuli. Due to excellent patterning ability of the DLW, LIG can be patterned and aligned in a way with a high freedom, which is beneficial to achieve complex shape transformation. Finally, theoretically DLW has unlimited lateral scanning region, resulting in ease scalability to meet application requirements. As potential applications, these self-morphing materials were demonstrated to: (1) produce programmable 3D shapes under multiple stimuli; (2) be used as soft grippers; and (3) fabricate soft robotics walking upon the various stimuli.

The fabrication process of the soft actuators was schematically represented in Fig. 1c

and described in the experimental section. First of all, the aligned LIG structures were produced on commercial PI films by a computer-controlled CO₂ laser.¹⁴ The DLW generates complex patterns such as a MU tiger logo (Fig. 1d). Under the scanning electron microscopy (SEM), the LIG show porous and aligned structures (Fig. 1e-f). According to the previous study, the porous structures result from the rapid liberation of gaseous products during the laser treatment.^{14, 22} The aligned structures are caused by the multiple scanning of the laser beam over the targeted areas, which forces the synthesized porous graphene to be aligned in a parallel orientation to the scanning direction of the laser beam (Fig. 1e).¹⁹ To better describe this aligned structure of the LIG, we define θ as the angle between the LIG orientation and the longitudinal direction of the resulting PLP films (Fig. S1). Such the aligned LIG is supposed to function as an anisotropic reinforcing element to control the self-morphing behaviors of the PLP actuators in the following experiments. By controlling the pathway of laser scanning, the LIG patterns with different alignment angles were obtained. After LIG fabrication, PVDF powder was dissolved in DMF and then was coated onto these LIG patterns. In order to improve heat transfer and mechanical coherence between the polymer layer and the LIG layer, strong interface is necessary. Normally, plasmas treatment can improve the interface between a polymer layer and a traditional non-porous carbon layer.²⁰ Thanks to the high porosity of the LIG structures, the PVDF solution can be easily infiltrated into the network of LIG to form strong PVDF/LIG interface directly without other additional physical or chemical treatment. After the DMF was evaporated on a hotplate, the LIG/PVDF bimorph was manually peeled off from the PI film (Fig. S2). It is noted that the peeled LIG/PVDF bimorph is naturally curved from LIG side to PVDF. This phenomenon is similar

to other reports when fabricating carbon/polymer bilayer films,²³ which may result from the strain mismatch between the LIG layer and the PVDF layer. To overcome this issue, a thin PI tape film was covered on the LIG side to neutralize the strain of LIG/PVDF and result in a flat film. Due to the physical adhesion of the PI tape film,²⁴ it can compact with LIG/ PVDF composite firmly as shown in Fig. S3. The PI film also acts passive layer in the resulting PLP actuator.

According to previous reports, LIG is a highly conductive material, which was used as an electrode material for a supercapacitor,¹⁴ strain sensor,¹⁹ photo detector,²⁵ electrocatalysts,²⁶ and artificial throat.²⁷ Due to its electrically conductive property, the LIG can efficiently convert electric energy into thermal energy, which makes it suitable a resistive heater for electrothermally active PLP actuators. In order to demonstrate this, we fabricated the LIG with a U-shape circuit pattern (Fig. 2a), which can guide the electric current to uniformly heat the PLP actuators. Copper electrodes were connected to two ends of U-shape circuit during the fabrication process. To evaluate electro-thermo-mechanical responses of the PLP actuators, we first fabricated the PLP actuators with LIG aligned in an alignment angle of 90°. The PLP actuators have width of 6 mm and length of 15 mm. The thicknesses of PVDF, LIG, and PI tape are $\sim 9 \mu\text{m}$, $45 \mu\text{m}$, and $25 \mu\text{m}$, respectively (Fig. S3). The resistances of the LIG electrodes is $\sim 300 \Omega$. The PLP actuators were connected to a direct current (DC) power supplier for electrical stimulation. When an input voltage of 14 V is applied to the PLP actuator, a quick bending movement from the PVDF side to the PI side is observed (Fig. 2a-b and Movie S1). After the electrical stimulation is retrieved, the bent PLP actuator returns to its initial flat state. This reversible response was investigated by evaluating

the time-dependent bending curvatures. As shown in Fig. 2c, the PLP actuator exhibits a bending curvature of 2.5 cm^{-1} in 5 s and recovers to a flat film in 10 s after the power is turned off. The energy efficiency of this electrothermal actuator was calculated as 0.028 %, which is comparable to previous works (method of calculating the energy efficiency is shown in Supporting Information)^{28, 29} In addition, the responsive behaviors of the PLP actuators under different voltages were also investigated (Fig. S4), which shows a higher voltage will lead to a faster response rate and a larger curvature.

These self-morphing behaviors of PLP actuators are driven by joule heat. As shown in Fig. 2d, the input voltage of 14 V leads to quickly increased temperature of the PLP actuator from 22 °C to 130 °C (Fig. 2c). And the higher voltage will result in higher temperature in the PLP actuators (Fig. S5). Due to the distinct thermal expansion coefficient of PVDF ($127 \times 10^{-6} \text{ K}^{-1}$)²⁰ and PI tape ($35 \times 10^{-6} \text{ K}^{-1}$),³⁰ the thermal expansion of PVDF is much larger than that of the PI tape, which results in bending from PVDF side to the PI side. It should be noted that such bending motion is well controlled by the alignment of LIG, in which the bending directions were always transverse to the alignment of LIG. This phenomenon can be attributed to the aligned structure of LIG. The LIG is believed to possess anisotropic mechanical property,¹⁹ in which it is stiffer in longitudinal direction (along the orientation of the aligned LIG) than it is in the transverse direction. Therefore, the expansion of the PVDF in the longitudinal direction is smaller than that in the transverse direction (Fig. 2e). Such constraining effect is observed in the PVDF/LIG bimorph upon heating (Fig. S6). As the temperature is increased from 25 to 120 °C, the PVDF/LIG bimorph exhibits thermal expansion of only 0.8% in the longitudinal direction (along the orientation of aligned LIG)

and $\sim 2.2\%$ in the transverse direction. This anisotropic expansion field makes the PLP actuators curve toward the transverse direction (Fig. 2f). In this case, the aligned LIG has the same function to the cellulose fibers in the plants, which can locally constrain the swelling of their surrounding matrix in the longitudinal direction where the fibers are aligned.

To further confirm the geometrical constraining role of LIG, actuators with $\theta = -45^\circ$ (Fig. 3a) and $+45^\circ$ (Fig. 3b) were fabricated. As expected, their responsive bending directions are also transverse to the alignment of LIG, which exhibit as right-handed helix and left-handed helix respectively. After understanding the basic responsive mechanism, we programmed a variety of complex 3D shapes. Even though bending and curling motions have been demonstrated on other electrothermal actuators,^{31, 32} they were usually shown in two separate actuators. It is still a challenge to achieve both motions in the same actuator. Herein, we realized both bending and curling motions in a single PLP actuator. This was achieved by patterning multiple LIG orientations with different alignment angles in one PI film. Fig. S7 shows optical images of LIG patterns with θ of 90° and 45° . Upon resistive heating, the bending and curling motions in the same PLP actuator were achieved. Different LIG patterns were fabricated to make the PLP actuators with varied actuation shapes. For instance, a three-armed electrothermal actuator was realized. The self-morphing behavior of each arm was well controlled by modulating θ as shown in Fig. 3c-3d and Movie S2-S3. Such three-armed actuator was used as a gripper to carry a plastic foam cargo (Fig. 3e and Movie S4). When a voltage is applied to the actuator, three arms bend and gather together to carry the cargo. When the voltage is turned off the arms release the cargo.

As a member of carbon nanomaterials, LIG also exhibits high absorption of light which

is then converted to thermal energy. Such photothermal effect can also drive the shape change of the PLP actuators. The photo responsive behavior of the PLP actuator was investigated by using a 150-W lamp as light source. The PLP actuators (2 mm x 15 mm) made from LIG aligned with $\theta = 90^\circ$ were first fabricated as a model. As shown in Fig. S8, a flat PLP actuator fast bends upon irradiation of the lamp at a distance of 4 cm from the actuator, and reaches a bending curvature of 1.8 cm^{-1} within 5 s. After the lamp is turned off, the actuator recovers to its original flat shape within 5.5 s. Such photo response can also generate a considerable mechanical force to lift a plastic foam that is > 20 times of its body weight (Fig. S9). Thermal images suggest that such bending is initiated by the photothermal heat (Fig. S10a). The mechanism of this photo responsive motion was similar as the aforementioned electrothermal one. The photo induced heat initiates asymmetrical thermal expansion in different layers of the PLP actuators and then causes the bending movement. Since the photo energy of the lamp is divergent, the light intensity received by the PLP actuator is related to the distance between the lamp and the PLP actuator. Thermal camera was used to record the temperature distribution of the PLP actuator when it is irradiated by the lamp from different distances. The results show that a smaller distance leads to a higher temperature in the PLP actuator (Fig. S10b), causing a larger bending curvature of the PLP actuator (Fig. 4a).

In addition, the photo responsive behavior is also programmable by varying the LIG alignment angles in the PLP actuators. As shown in Fig. S11, the PLP actuators (2 mm x 15 mm) with $\theta = -45^\circ$ and 45° exhibit right-handed and left-handed helices under irradiation of the lamp, confirming that LIG structures enable to control curling direction of the PLP actuators. We also fabricated the PLP actuators that can evolve into different geometries. For

instance, we demonstrated a flower shape with a LIG alignment angle of 90° in each petal (Fig. 4b). By switching on and off the lamp, this flower-shaped PLP actuator reversibly close and open the petals. We also fabricated an identical pattern, but the LIG alignment angle in the petals was changed from 90° to $+45^\circ$ (Fig. 4c). In this case, the PLP actuator evolves into a curled flower-shape under irradiation of the lamp (Movie S5). To explore the application of the PLP actuator, we present a photo actuated mm scale robot, whose motion directions can be well controlled. As shown in Fig. 4d, the mm scale robot consists five legs made from LIG with alignment angle of 90° . When the robot is irradiated by the lamp laterally, the five legs receive different photon energy because of their different distances to the lamp, causing various bending curvatures in each leg. The legs which are closer to the lamp are highly bent, while the farther legs is less bent (Fig. 4d). When lamp is turned off, the highly bent legs recover to its original flat configuration, causing friction force between the legs and the substrate. This force drives the mm scale robot to move forward along the same direction of light. By switching on and off the lamp, the soft robot continuously moves forward by repeating the cycle (Movie S6). Compared to previously reported photosensitive microrobots, which often have simple configuration and only moves in one direction,²³ our robot exhibits more complex configuration and moves in multiple but controllable directions. As shown in Fig. 4e and Movie S7, when the irradiation direction of the lamp is changed, the legs oriented in different positions are activated, which results in movement in different directions. This interesting characteristics of multi-directional movement in the PLP mm scale robots show that LIG structures tailored by the simple DLW process can efficiently modulate the device performance, paving a new route to soft robotics. In addition, a self-sensing actuator was also

demonstrated on a PLP actuator, in which the PLP actuator can be used as a sensor to simultaneously monitor the bending deformation of itself.³³ We firstly fabricated the PLP actuator with a U-shape circuit pattern. Then a crease was made on LIG by a knife (Figure S12a), which caused bad connections between LIGs in the crease area to purposely increase the electrical resistance of LIG. When the PLP actuator was exposed to light, the bad connection of LIG is reconnected due to the thermal expansion of PVDF/LIG (Figure S12b), which results in a smaller resistance of LIG (Figure S12c). The resistance values and bending curvatures of PLP actuator changed simultaneously when exposed to a light source (Movie S8). Therefore, the resistance values of LIG can be recorded as an indicator to monitor the photothermal actuation of PLP actuators (Figure S12d).

Besides responding to the heat induced by the electrical and photon energy, the resulting PLP actuators are also responsive to chemical stimulation. Our previous results show that the PVDF has a strong swelling ability toward organic solvents such as acetone.²¹ When stimulated by acetone, the PLP actuator bends from the side of PVDF to the side of the PI due to their asymmetrical swelling ratios (Fig. 5a). The role of the aligned LIG is to induce anisotropic strains in different directions of the PVDF. This conclusion is proved by the results shown in Fig. S13. Upon acetone stimulation, the expansion strain (4.9%) in the transverse direction is much larger than that in the longitudinal direction (1.8%). Two PLP actuators with different LIG alignment angles were fabricated (Fig. 5b and 5c). They exhibit reversible closing/opening motions (Fig. 5b) or twisting/untwisting motions (Fig. 5c and Movie S9) upon the stimulation of acetone vapor (30 kPa, 25 °C).³⁴ In addition, the demonstrated device architecture can be applied to different polymeric systems. For instance,

if the PVDF is replaced by polyvinyl alcohol (PVA), a hydrophilic polymer which has a large swelling upon uptaking moisture,³⁵ a PLP actuator that is based on PVA/LIG/PI is responsive to water or moisture. As shown in Fig. 5e and 5f, a PVA/LIG/PI flower made from a LIG film aligned in different alignment angles exhibits programmable shape transformation (closing and twisting) when stimulated by the moisture evaporating from human's hand (relative humidity is about 50%).³⁶ It also acts as a humidity-driven soft gripper (Fig. 5g and Movie S10). The gripper is placed above a targeted object. After water is sprayed on its surface, the petals of the gripper close and capture the object in ~2 min. When the object is moved to a desired location, light irradiation is used to evaporate the water in the PVA/LIG/PI gripper. The petals recover to their original shapes and release the object.

In summary, we report a bottom-up approach to fabricate aligned LIG whose microstructures mimic the cellulose fibrils in the plants as geometrically constraining elements for responsive materials. These bio-mimic structures can be designed and tailored with different alignment angles, resulting in a series of programmable actuators which respond to electric, light, organic vapor, and moisture. These PLP actuators are superior to the state-of-art multi-responsive soft actuators in terms of response speed to various stimuli (Table S1).^{28, 37} Multiple types of shape changing behaviors, from bending to helical curling, were demonstrated on these actuators by tuning the structures of LIG. These tailored structures and their resulting devices show potentials of being adapted to a wide range of applications such as sensing, artificial muscles, and soft robotics. Given that DLW is a scalable process, the demonstrated devices can be mass produced for widespread applications. The present study also provides a new route to other responsive polymer systems with

different material structures and responsive characteristics.

Supporting Information

Electronic supplementary information (ESI) available

Conflict of Interest

The authors declare no conflict of interest

Acknowledgements

The work was supported by University of Missouri-Columbia start-up fund, NASA Missouri Space Consortium (Project: 00049784), NASA Goddard Space Flight Ctr. (Project: 00057234), NSF SBIR program (Award number: 1648003), and United States Department of Agriculture (Award number: 2018-67017-27880).

References

1. C. Dawson, J. F. Vincent and A.-M. Rocca, *Nature*, 1997, **390**, 668.
2. S. Armon, E. Efrati, R. Kupferman and E. Sharon, *Science*, 2011, **333**, 1726-1730.
3. R. Elbaum, L. Zaltzman, I. Burgert and P. Fratzl, *Science*, 2007, **316**, 884-886.
4. R. M. Erb, J. S. Sander, R. Grisch and A. R. Studart, *Nat. Commun.*, 2013, **4**, 1712.
5. H.-W. Huang, M. S. Sakar, A. J. Petruska, S. Pané and B. J. Nelson, *Nat. Commun.*, 2016, **7**, 12263.
6. Y. Liu, B. Xu, S. Sun, J. Wei, L. Wu and Y. Yu, *Adv. Mater.*, 2017, **29**, 1604792.
7. A. S. Gladman, E. A. Matsumoto, R. G. Nuzzo, L. Mahadevan and J. A. Lewis, *Nat. Mater.*, 2016, **15**, 413-418.
8. J. Deng, J. Li, P. Chen, X. Fang, X. Sun, Y. Jiang, W. Weng, B. Wang and H. Peng, *J. Am. Chem. Soc.*, 2015, **138**, 225-230.
9. L. Zhang, S. Chizhik, Y. Wen and P. Naumov, *Adv. Funct. Mater.*, 2016, **26**, 1040-1053.
10. D. Morales, B. Bharti, M. D. Dickey and O. D. Velev, *Small*, 2016, **12**, 2283-2290.

11. H. Peng, X. Sun, F. Cai, X. Chen, Y. Zhu, G. Liao, D. Chen, Q. Li, Y. Lu and Y. Zhu, *Nat. Nanotechnol.*, 2009, **4**, 738.
12. H. E. McFarlane, A. Döring and S. Persson, *Annu. Rev. Plant Biol.*, 2014, **65**, 69-94.
13. C. Somerville, *Annu. Rev. Cell Dev. Biol.*, 2006, **22**, 53-78.
14. J. Lin, Z. Peng, Y. Liu, F. Ruiz-Zepeda, R. Ye, E. L. Samuel, M. J. Yacaman, B. I. Yakobson and J. M. Tour, *Nat. Commun.*, 2014, **5**, 5714.
15. L. Xuan and J. M. James, *Carbon*, 2017, **126**, 472-479.
16. J. Zhang, M. Ren, Y. Li and J. M. Tour, *ACS Energy Lett.*, 2018, **3**, 677-683.
17. R. Ye, X. Han, D. V. Kosynkin, Y. Li, C. Zhang, B. Jiang, A. A. Marti and J. M. Tour, *ACS nano*, 2018, **12**, 1083-1088.
18. H. Deng, C. Zhang, Y. Xie, T. Tumlin, L. Giri, S. P. Karna and J. Lin, *J. Mater. Chem. A*, 2016, **4**, 6824-6830.
19. R. Rahimi, M. Ochoa, W. Yu and B. Ziaie, *ACS Appl. Mater. Inter.*, 2015, **7**, 4463-4470.
20. Y. Tai, G. Lubineau and Z. Yang, *Adv. Mater.*, 2016, **28**, 4665-4670.
21. H. Deng, Y. Dong, C. Zhang, Y. Xie, C. Zhang and J. Lin, *Mater. Horiz.*, 2018, **5**, 99-107.
22. Y. Dong, S. C. Rismiller and J. Lin, *Carbon*, 2016, **104**, 47-55.
23. Y. Hu, G. Wu, T. Lan, J. Zhao, Y. Liu and W. Chen, *Adv. Mater.*, 2015, **27**, 7867-7873.
24. C. Wang, K. Sim, J. Chen, H. Kim, Z. Rao, Y. Li, W. Chen, J. Song, R. Verduzco and C. Yu, *Adv. Mater.*, 2018, **30**, 1706695.
25. C. Zhang, Y. Xie, H. Deng, T. Tumlin, C. Zhang, J. W. Su, P. Yu and J. Lin, *Small*, 2017, **13**, 1604197.
26. R. Ye, Z. Peng, T. Wang, Y. Xu, J. Zhang, Y. Li, L. G. Nilewski, J. Lin and J. M. Tour, *ACS nano*, 2015, **9**, 9244-9251.
27. L.-Q. Tao, H. Tian, Y. Liu, Z.-Y. Ju, Y. Pang, Y.-Q. Chen, D.-Y. Wang, X.-G. Tian, J.-C. Yan and N.-Q. Deng, *Nat. Commun.*, 2017, **8**, 14579.
28. M. Amjadi and M. Sitti, *ACS nano*, 2016, **10**, 10202-10210.
29. L. Chen, M. Weng, W. Zhang, Z. Zhou, Y. Zhou, D. Xia, J. Li, Z. Huang, C. Liu and S. Fan, *Nanoscale*, 2016, **8**, 6877-6883.
30. M. Ree, K. J. Chen, D. Kirby, N. Katzenellenbogen and D. Grischkowsky, *J. Appl. Phys.*, 1992, **72**, 2014-2021.
31. Z.-w. Zhou, Q.-h. Yan, C.-h. Liu and S. Fan, *New Carbon Mater.*, 2017, **32**, 411-418.
32. L. Chen, C. Liu, K. Liu, C. Meng, C. Hu, J. Wang and S. Fan, *ACS nano*, 2011, **5**, 1588-1593.
33. M. Amjadi and M. Sitti, *Adv. Sci.*, 2018, 1800239.
34. Q. Zhao, J. W. Dunlop, X. Qiu, F. Huang, Z. Zhang, J. Heyda, J. Dzubiella, M. Antonietti and J. Yuan, *Nat. Commun.*, 2014, **5**, 4293.
35. L. Zhang, I. Desta and P. Naumov, *Chemical Communications*, 2016, **52**, 5920-5923.
36. R. Mole, *J. Physiol.*, 1948, **107**, 399-411.
37. M. Weng, P. Zhou, L. Chen, L. Zhang, W. Zhang, Z. Huang, C. Liu and S. Fan, *Adv. Funct. Mater.* 2016, **26**, 7244-7253.

Figure legends

Fig. 1 (a) Schematic of aligned cellulose fibril in botanic systems and their function of controlling actuation of plants upon water uptake. (b) Schematic of aligned LIG by DLW and their function of controlling actuation of resulting soft actuators. (c) Schematic of fabrication process for a PVDF/LIG/PI actuator. (d) Photograph of a patterned Mizzou tiger logo composed of LIG. (e)-(f) SEM images of LIG.

Fig. 2 (a) Top-view photographs of a PLP actuator with $\theta = 90^\circ$ showing reversible actuation by electric stimulation. (b) Side-view photographs of a PLP actuator with $\theta = 90^\circ$ under electric stimulation. (c) Plot of bending curvatures of a PLP actuator as a function of time. (d) Thermal images of a PLP actuator when electric stimulation is on and off. (e) Schematic of a PVDF/LIG bimorph showing anisotropic thermal expansion. (f) Schematic of a PLP actuator showing shape transformation behaviors due to the anisotropic thermal expansion of the PVDF/LIG bimorph.

Fig. 3 (a) Top-view photographs of a PLP actuator with $\theta = -45^\circ$ when electric stimulation is on and off. (b) Top-view photographs of a PLP actuator with $\theta = +45^\circ$ when electric stimulation is on and off. (c) Top-view photographs of a three-armed PLP actuator with $\theta = 90^\circ$ when electric stimulation is on and off. (d) Top-view photographs and thermal images of a three-armed PLP actuator with $\theta = -45^\circ$ under electric stimulation. (e) Photographs of a PLP soft gripper delivering a cargo under electric stimulation.

Fig. 4 (a) Photographs of a PLP actuator upon exposure to light with different distances. **(b)-(c)** Photographs of a flower-shaped PLP actuator with **(b)** $\theta = 90^\circ$ and **(c)** $\theta = +45^\circ$ when exposed to light. **(d)** Photographs of a PLP robot crawling by switching the light on and off. **(e)** Schematic and photographs of a PLP robot with multi-ways gaits under light stimulus.

Fig. 5 (a) Schematic of a PLP actuator under stimulation of acetone. **(b)-(c)** Photographs of PLP trefoils with **(b)** $\theta = 90^\circ$ and **(c)** $\theta = -45^\circ$ under stimulation of acetone. **(d)** Schematic of a PVA/LIG/PI actuator under stimulation of water. **(e)-(f)** Photographs of PVA/LIG/PI flower-shaped actuators with **(e)** $\theta = 90^\circ$ and **(f)** $\theta = -45^\circ$ under stimulation of moisture from hand. **(g)** Photographs of a PVA/LIG/PI soft gripper delivering a cargo by water stimulation.

Fig. 2

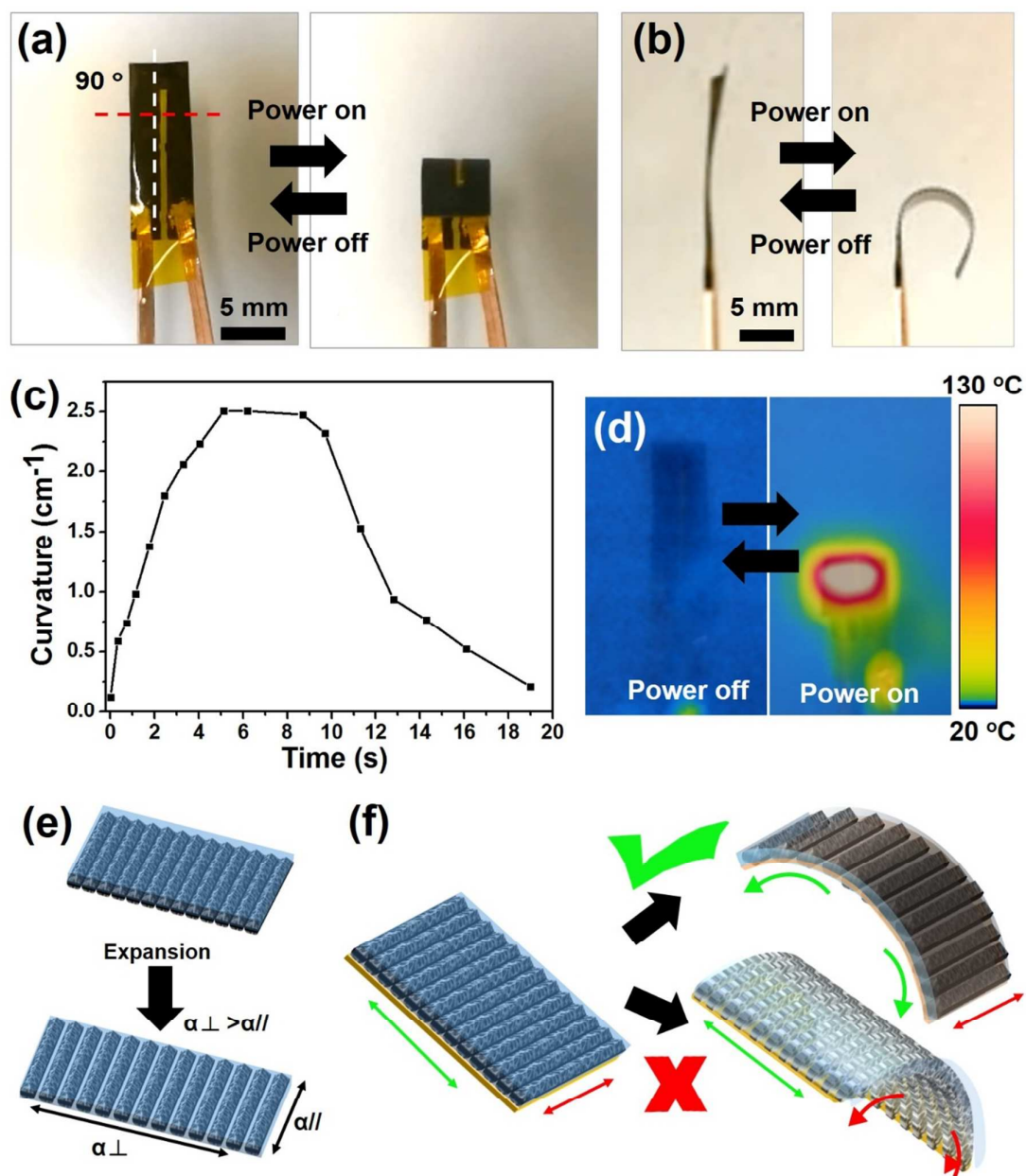


Fig. 3

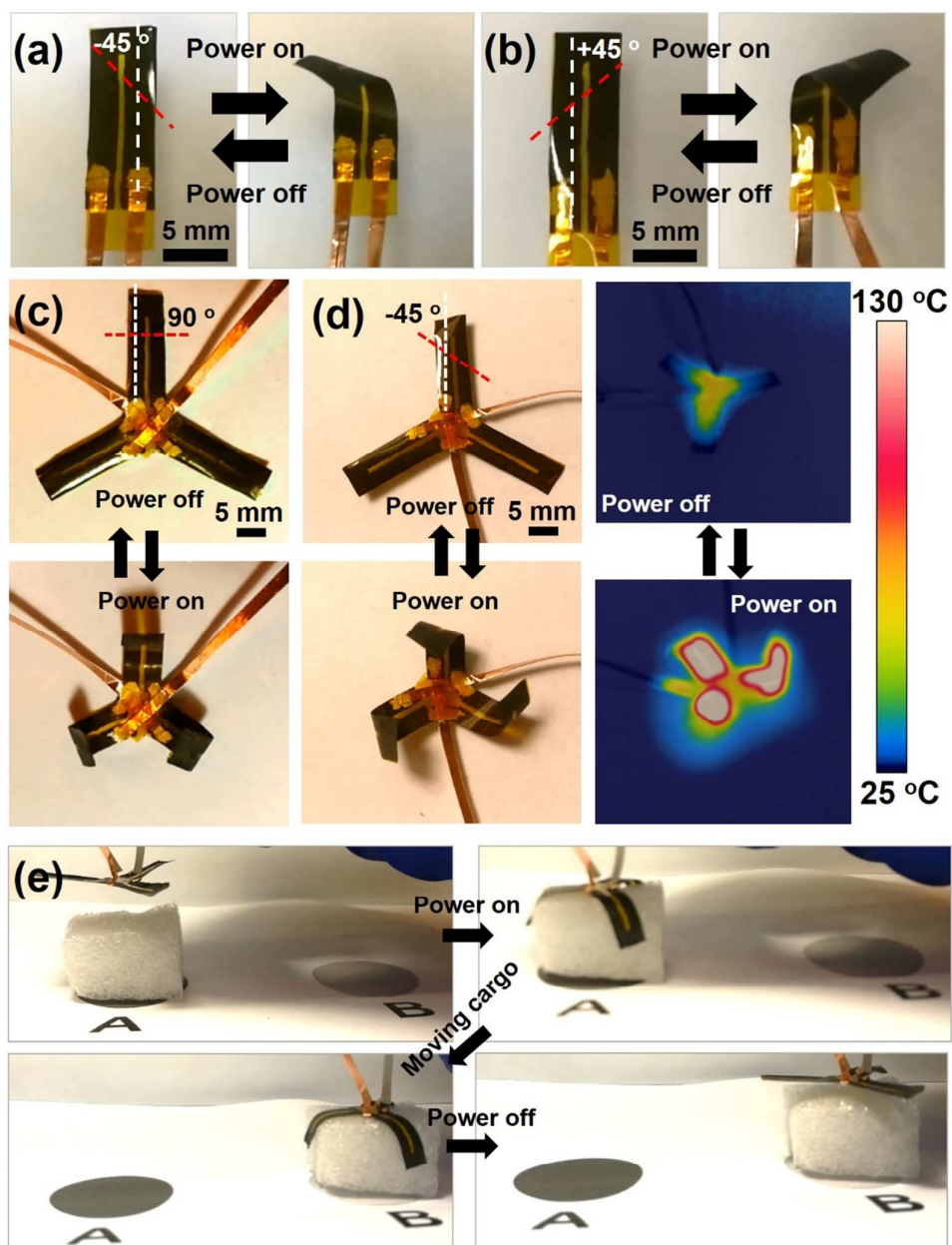


Fig. 4

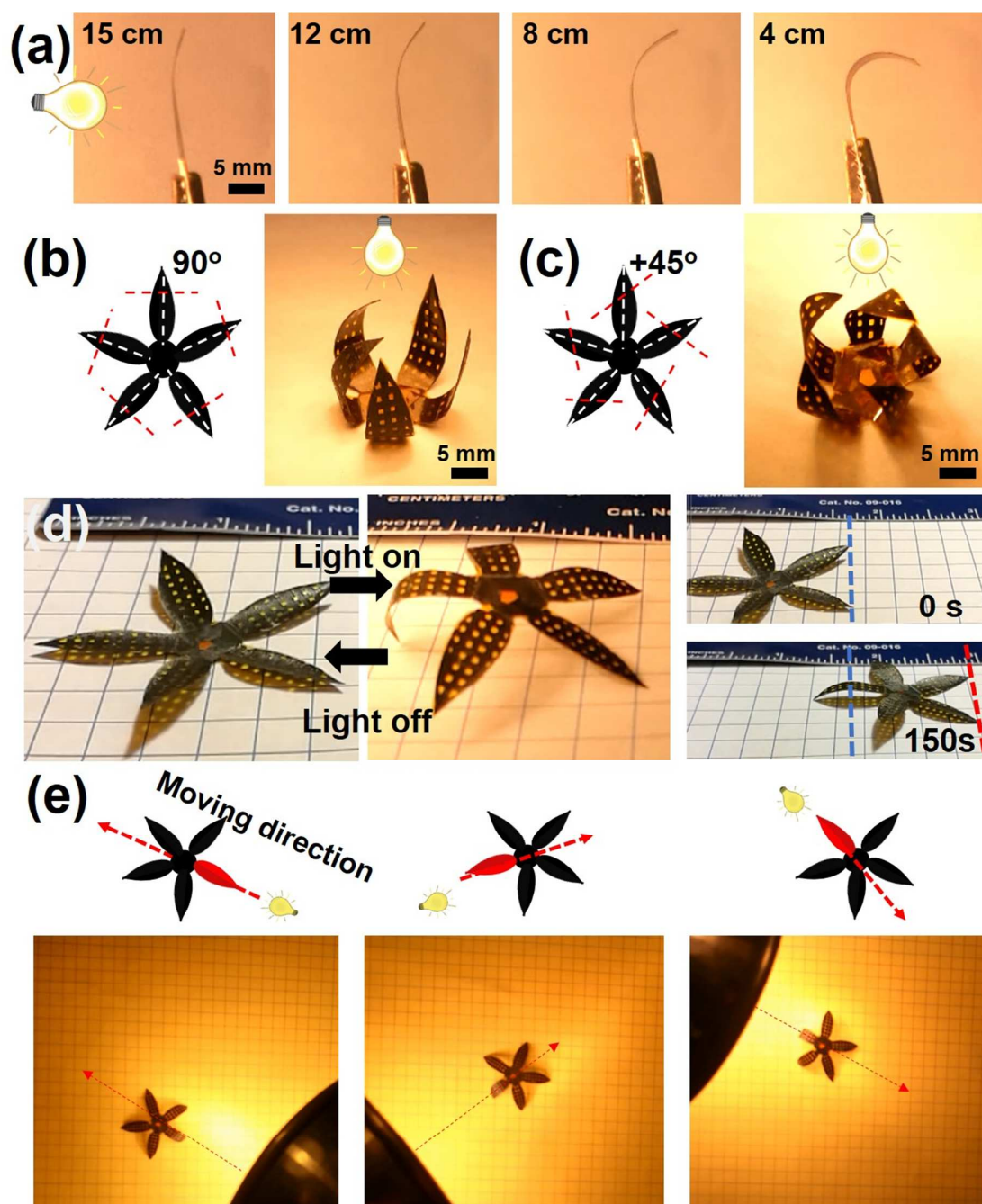


Fig. 5

